Middle Miocene paleoaltimetry of southern Tibet: Implications for the role of mantle thickening and delamination in the Himalayan orogen

Brian S. Currie Department of Geology, 114 Shideler Hall, Miami University, Oxford, Ohio 45056, USA
David B. Rowley Department of the Geophysical Sciences, 5734 South Ellis Avenue, University of Chicago, Chicago, Illinois 60637, USA
Neil J. Tabor Department of Geological Sciences, Southern Methodist University, Dallas, Texas 75275, USA

ABSTRACT

The stable isotope composition of pedogenic and early diagenetic carbonates from the Oiyug Basin of southern Tibet allows model estimates of the paleoaltimetry of the Tibetan Plateau for the middle Miocene. Pedogenic calcium carbonate nodules have average $\delta^{18}O_{cc}$ values of −19.6‰, whereas nodular lacustrine dolomites range in composition from −7.6‰ to −5.5‰. The most negative of the carbonate isotope values can be used to constrain the oxygen isotope composition of paleoprecipitation, from which model estimates of paleoaltimetry can be made. Model results indicate that the southern Tibetan Plateau achieved elevations of ~5200 +1370/−605 m by at least 15 Ma. Our results are identical within uncertainty to previous workers' paleoelevation estimates based on Oiyug Basin fossil floral physiognomy. This is the first time that two paleoaltimeters have been directly compared and are in accord. Collectively, these data strongly support tectonic models in which thickening of mantle lithosphere beneath the domain of crustal thickening and subsequent detachment of the mantle lithosphere plays an indiscernible role in the elevation history of this part of the Himalaya-Tibet orogenic system.

Keywords: Tibetan Plateau, paleoelevation, oxygen isotopes, middle Miocene.

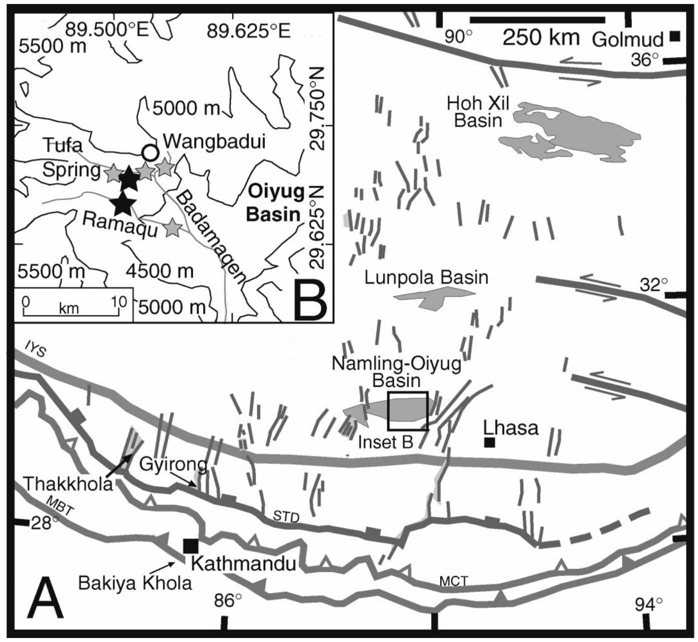

Figure 1. A: Location map of Tibetan basins from which paleoelevation estimates have been derived. B: Location map of Oiyug Basin samples described in text. Only streams and rivers mentioned in text are highlighted. Large black stars are carbonate nodule localities. Northern black star also corresponds with Miocene floral locality described by Spicer et al. (2003). Gray stars are sample localities for modern surface waters, including tufa spring west of Wangbadui. Abbreviations: IYS—Indus-Yarlung suture; STD—South Tibetan detachment; MBT—Main Boundary thrust; MCT—Main Central thrust.

INTRODUCTION

The uplift history of the Tibetan Plateau has been a focus of considerable interest since Argand (1924) first proposed that the plateau resulted from the collision and underthrusting of India beneath Asia to double the crustal thickness of this region. Subsequent workers developed alternative models for the tectonic evolution of Tibet (see Harrison et al., 1992). Molnar et al. (1993) proposed an appealing model integrating observations from geodynamics to paleoclimatology, in which uplift of Tibet took place in two stages. The first stage, dating from the initiation of collision at 50 Ma (Bin et al., 2005) to ca. 10–8 Ma, resulted in bulk shortening and thickening of the crust and mantle lithosphere to produce a plateau of ~3 km average elevation. According to this model, ca. 8 Ma the mantle lithosphere became gravitationally unstable and detached, replacing denser mantle lithosphere with less dense asthenospheric mantle, leading to regional isostatic uplift of the plateau by an additional 2 km to an average elevation of 5 km. The appeal of this model has been that it directly linked a wide spectrum of processes and events, including (1) onset of the Asian monsoon, (2) onset of upwelling off the Somalian margin, (3) transition from C_3 to C_4 grasses in Pakistan, (4) east-west extension across the Himalaya and Tibet, and (5) north-south shortening in the Indian oceanic lithosphere south of India. Other models, including those of Argand (1924), Dewey and Burke (1973), and Beaumont et al. (2004), focus entirely on mechanisms of crustal thickening. Beaumont et al. (2004) used a thermo-mechanical model of crustal deformation to make explicit predictions about the elevation history and large-scale structural geometry based on parameters that accord well with observed convergence rate and crustal thickness of the Himalaya-Tibet system. An important facet of all of these models is that they make either implicit or, in the cases of Molnar et al. (1993) and Beaumont et al. (2004), explicit predictions regarding the elevation history of the plateau that can be tested.

Until recently, quantitative techniques to estimate paleoelevation did not exist; direct tests of the various models of the evolution of orogenesis were therefore not possible. Rowley et al. (2001) provided the physical and thermodynamic basis of a model that uses oxygen and hydrogen isotopes in precipitation in low-latitude (<35°) orographic systems to estimate paleoelevations and, potentially, paleohypsometries. Rowley et al. (2001) used data from the Thakkhola and Gyirong Basins (Fig. 1A), the oldest intermontane basins within the Himalayas, to demonstrate that the Himalayas attained their current stature at least since 10–8 Ma. Garzione et al. (2000), using empirically derived calibrations, arrived at a similar conclusion.

Rowley et al. (2001) derived the expected relationship between $\Delta(\delta^{18}O_p)$ and elevation based on atmospheric thermodynamics and Rayleigh distillation of orographically forced ascent of air masses. The $\Delta(\delta^{18}O_p)$ value is the difference between the oxygen isotope composition of precipitation falling to the ground at elevation and at sea level. The results of integrating the equations governing the relationship between $\Delta(\delta^{18}O_p)$ and elevation using the probability density function for low-latitude temperature and relative humidity were only presented graphically in Rowley et al. (2001). The relationship between $\Delta(\delta^{18}O_p)$, for values of $\Delta(\delta^{18}O_p)$ between 0.0‰ and −40.0‰, and elevation (h) in meters graphed in Rowley et al. (2001) can be described by the polynomial fit in equation 1.

$$h = (-6.14 \times 10^{-3})\Delta(\delta^{18}O_p)^4 - 0.6765\Delta(\delta^{18}O_p)^3 - 28.623\Delta(\delta^{18}O_p)^2 - 650.66\Delta(\delta^{18}O_p). \quad (1)$$

Rowley et al. (2001) discussed in some detail sources of uncertainty and highlighted the primary factors controlling the relationship between $\Delta(\delta^{18}O_p)$ and elevation, i.e., starting low-elevation temperature and relative humidity. A probability density function of low-latitude temperature and relative humidity was used to assess uncertainties, and we use those results in our discussion.

Spicer et al. (2003) used physiognomic characteristics of a fossil flora (ca. 15 Ma) from the Namling-Oiyug Basin of southern Tibet (Figs. 1A, 1B) to estimate paleoenthalpy of the atmosphere within which the flora grew. The flora was dated by Spicer et al. (2003) as ca. 15 Ma. By coupling their paleoenthalpy value with general circulation model–derived paleoenthalpy values for the lowland region immediately south of their locality, they were able to estimate the 15 Ma elevation of the Oiyug floral locality as 4650 ± 875 m. Spicer et al. (2003) thus provided the first quantitative estimate to suggest that (1) southern Tibet was higher than predicted by the Molnar et al. (1993) model in the middle Miocene and (2) this region of Tibet has not changed its elevation since these floras existed.

In this paper we report the stable isotope compositions of modern stream and hydrothermal waters collected near the sample locality reported by Spicer et al. (2003) as well as estimates of stable isotope compositions of paleowater derived from Miocene soil carbonate nodules from strata below the fossil flora locality. Rowley et al. (2001) used published data on the modern waters from southern Tibet and the Himalaya as an independent test of the theoretical model developed in their paper (see references cited therein). The stable isotopic compositions of modern waters from the Oiyug Basin provide a further test of the model of Rowley et al. (2001), and the paleosol carbonate nodules allow a comparison with the floral-based paleoenthalpy approach used by Spicer et al. (2003).

MODERN WATERS AND ESTIMATING PRESENT ELEVATIONS

Stream waters were collected in November 2000 from the Badamaqen and an unnamed tributary near the village of Wangbadui (~29.7°N, 89.5°E) as well as the Ramaqu to the south (29.65°N, 89.55°E) (Fig. 1B). Water was also collected from a tufa spring (29.7125°N, 89.5792°E) west of Wangbadui and upstream from the Spicer et al. (2003) floral locality (Fig. 1B). Waters from the Badamaqen and associated tributaries were also collected in April 2000 by Nigel Harris during the collection of the floral samples studied by Spicer et al. (2003). Oxygen isotope compositions of the stream samples are listed in Figure 2.

The samples were collected at elevations between 4350 m and ~4450 m; maximum elevations adjacent to this part of the Oiyug Basin are ~5600 m. Equation 1 was used to predict elevations for each of the modern water samples; the $\Delta(\delta^{18}O_p)$ value used was based on (1) the sample's measured $\delta^{18}O_w$ value, which integrates $\delta^{18}O_p$ of the drainage basin above the sample elevation, and (2) the assumption of a low-elevation $\delta^{18}O_p$ value of −5.8‰ (derived from precipitation data from New Delhi [International Atomic Energy Agency, 1992]). The

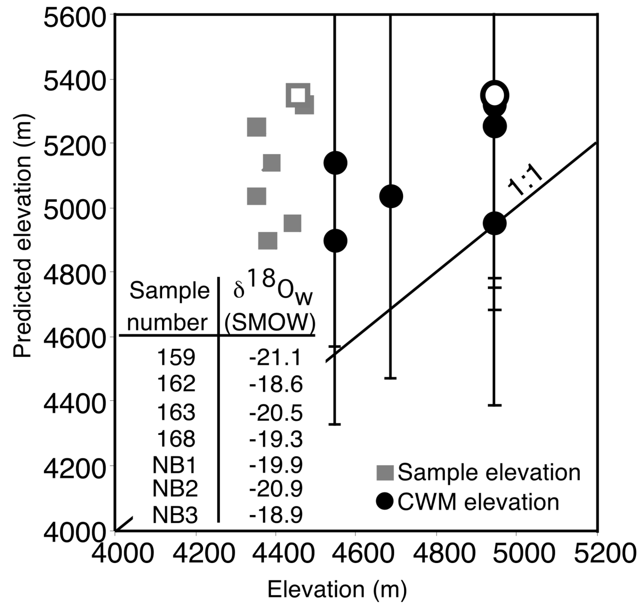

Figure 2. Sample and condensation-weighted mean (CWM) elevations vs. oxygen isotope–based predicted elevations for samples from within Oiyug Basin (locations shown in Fig. 1B). Squares—modern sample elevations (based on combined global positioning system and barometric pressure–derived estimates of elevation) vs. oxygen isotope–predicted elevations. Circles—CWM elevations (derived from Globe v. 1.0 30 s digital elevation model) of drainage basins above present-day sample sites. Open symbols—hot tufa springs. Uncertainties in predicted elevation are from Rowley et al. (2001). SMOW—standard mean ocean water.

$\delta^{18}O_w$ values of streams should correlate better with the higher hypsometric mean elevation than with the sample elevation. There is typically an even better correlation with condensation-weighted hypsometric mean (CWM) elevation of the drainage basin because the amount of condensation of water vapor to form precipitation also varies with elevation. The CWM weights the hypsometry of the drainage basin above the sample elevation by the amount of condensation in the atmosphere per increment of elevation change. Figure 2 shows the correlations of both sample elevation and CWM elevations vs. the oxygen isotope–based predicted elevations. Although the correlation is not perfect, with an average difference between the CWM and predicted elevation of <350 m, it is clear that relative to the model uncertainties (+1300/−600 m) the deviations are small and systematic. It is possible that the systematic offset to higher predicted elevation than expected reflects distillation due to rainout before reaching the Wangbadui area either as a consequence of the distance traveled or having encountered higher elevations along the air-mass trajectory. Nonetheless, these results together with the previous analysis of modern waters reported by Rowley et al. (2001) suggest that the model captures the main processes responsible for isotopic fractionation of precipitation in this orographic setting. The tufa spring (open symbols), which represents a part of the groundwater system, also reflects derivation from the local precipitation.

ESTIMATES OF MIOCENE PALEOELEVATION

Along the western flank of the Oiyug Basin, ~3 km of Cenozoic strata are exposed in a southeast-dipping section (Fig. 1B). The focus of our investigation was on ~400 m of fluvial, alluvial, lacustrine, and volcanic strata cropping out west of the village of Wangbadui and in the valley of the Ramaqu River (Fig. 3). The section consists of a lower unit of ~200 m of variegated sandstones and mudstones that contain fluvial, alluvial, and lacustrine facies. This lower unit is overlain by

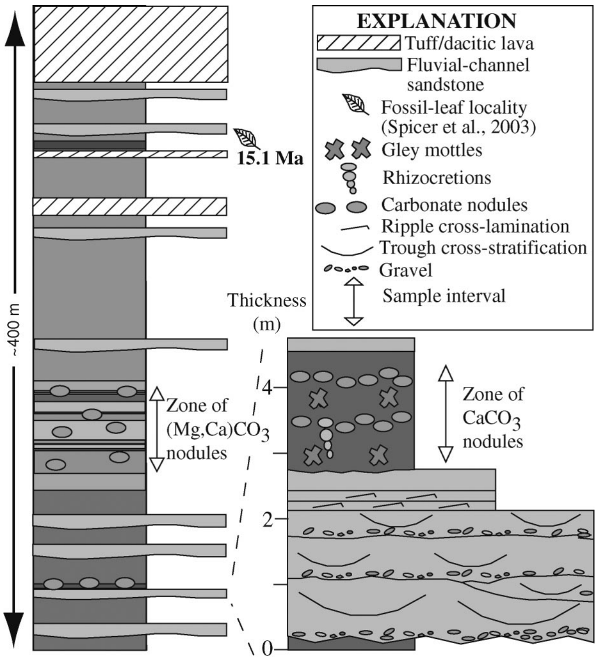

Figure 3. Composite stratigraphic section of Miocene sequence exposed along Ramaqu River (locations in Fig. 1B), showing relationships among primary sequences and sampled horizons. Age of 15.1 Ma for tuffaceous bed below floral locality in section is $^{40}Ar/^{39}Ar$ age of Spicer et al. (2003).

~200 m of sandstone, carbonaceous mudstones, and intercalated tephra. Dating ($^{40}Ar/^{39}Ar$) of tuffs near the top of this interval indicates a 15.1 Ma age of deposition (Spicer et al., 2003). This date provides a minimum middle Miocene age for deposition of the studied interval.

As part of this study we collected carbonate nodules from an ~2-m-thick zone of alluvial paleosols overlying a fluvial-channel sandstone in the lower part of the lower variegated unit (Fig. 3). The upper horizon of the paleosol interval consists of gray, noncalcareous, structureless, sandy mudstone that grades downward to a reddish-brown clay-rich horizon that displays medium to very coarse, subangular to angular blocky ped structures. This clay-rich horizon (Bt horizon, Brewer, 1976) contains argillans along ped surfaces. Underlying this argillic horizon are carbonate nodules and vertical rhizocretions (Btk, Bk horizons). Nodules range from a few millimeters to as much as 3 cm in diameter and define discrete calcareous horizons (stage III–IV; Machette, 1985) as much as 35 cm thick. Nodules grade downward into the Bt horizon of an underlying paleosol with a similar morphology. The lower horizon of each paleosol contains green-gray gley mottles. We interpret these paleosols as a series of stacked argillic Calcisols (sensu Mack et al., 1993). Both the argillic and calcic horizons in the paleosols are interpreted to have formed as a result of translocation of authigenic clays and leaching of calcium carbonate from upper soil horizons by meteoric water during pedogenesis. Carbonate nodules sampled for this study were taken from >40 cm below interpreted surface horizons.

Dolomite nodules were collected from lacustrine mudstones and dolomitic marls in the upper part of the variegated unit, ~75–120 m above the calcic paleosols described here (Fig. 3). These nodules are as much as 30 cm in diameter and are characterized by structureless, very finely crystalline dolomite that contains small particles of the host lithologies. In some instances laminations in surrounding mudstones are differentially compacted, indicating that the nodules formed prior to lithification of the host deposits. None of the nodular horizons is associated with morphological features indicative of pedogenesis. We interpret the nodular dolomites as being early-diagenetic phreatic carbonates. The close association with lacustrine mudstones and dolomitic marls suggests that these nodules may have formed in lake-margin settings during seasonal fluctuations in lake level (e.g., Calvo et al., 1989).

Pedogenic calcium carbonate nodules have average $\delta^{18}O_{cc}$ (Vienna Peedee belemnite) values of −19.6‰ and $\delta^{13}C_{cc}$ values of −6.8‰. The $\delta^{18}O_d$ values of the nodular dolomites range from −7.6‰ to −5.5‰, and their $\delta^{13}C_d$ values range from −7.3‰ to −5.1‰. The wide range of $\delta^{18}O$ values from the dolomite nodules most likely reflects evaporative enrichment of basin groundwater during the time of nodule formation. As such, the most negative samples are likely closest to the original isotopic composition of meteoric waters at the time of carbonate precipitation.

The $\delta^{18}O$ value of authigenic carbonates, such as those sampled from the Oiyug Basin, has been used as proxies for the composition of meteoric water (Kelts and Talbot, 1989; Cerling and Quade, 1993; among others). By using the fractionation factors for calcite-water and dolomite-water determined by Friedman and O'Neil (1977) and the paleo–mean annual temperature (MAT) of 6.8° ± 3.4 °C determined by the Spicer et al. (2003) leaf-margin analysis of the Namling flora, we estimated the $\delta^{18}O$ value of paleometeoric water ($\delta^{18}O_w$). The pedogenic calcite nodules described here precipitated from meteoric water with a $\delta^{18}O_w$ value of −21.7‰ ± 1.7‰ (Vienna standard mean ocean water, VSMOW). Similarly, the most negative of the nodular dolomites precipitated from groundwater that had a $\delta^{18}O_w$ value of −15.6‰ ± 3.6‰ (VSMOW).

The difference in $\delta^{18}O_p$ between high- and low-elevation localities ($\Delta\delta^{18}O_p$) provides the basis for the calculations of paleoaltitude using the model of Rowley et al. (2001). For our low-altitude reference, we use $\delta^{18}O_{cc}$ values of pedogenic carbonates from the middle Miocene Siwalik Group (ca. 17–14 Ma) of northern Pakistan that yield mean values of −9.5‰ ± 1.3‰ (Cerling and Quade, 1993). Assuming a MAT of 25 °C, we estimate a low-elevation $\delta^{18}O_p$ value of −7.2‰ (VSMOW) for middle Miocene paleoprecipitation. The effect of normalizing our estimate of $\delta^{18}O_p$ with the middle Miocene Siwalik value relative to the ~−6‰ value of today is to reduce predicted elevations. Given these values, our best estimate of middle Miocene $\Delta(\delta^{18}O_p)$ derived from pedogenic calcite nodules from the Himalayan foreland and the Oiyug Basin is −14.5‰ ± 2.1‰ (VSMOW). The uncertainty reflects combined contributions of the low-elevation $\delta^{18}O_p$ value (±1.3‰) and the temperature at which carbonate and water were in equilibrium during carbonate precipitation (±1.7‰). The predicted CWM elevation corresponding with a $\Delta(\delta^{18}O_p)$ value of −14.5‰ ± 2.1‰ is ~5200 m +340/−405 (Fig. 4). The uncertainty in the elevation estimate corresponds to the 1 sigma (1σ) standard deviation in $\Delta(\delta^{18}O_p)$. The additional source of uncertainty in the predicted elevation arising from temperature and relative humidity variation in the starting air mass prior to any rain-out effect as described in Rowley et al. (2001) results in ±1σ model uncertainty associated with a $\Delta(\delta^{18}O_p)$ value of −14.5‰ of ~+1370/−600 m (Fig. 4).

Global climate change since the middle Miocene is thought to have resulted in reduced global temperatures. Warmer and more humid mean climate would lead to a higher estimate of paleoelevation, reflecting the fact that Rayleigh distillation associated with orographic lift would be less efficient because there would be less condensation at lower elevations (Rowley et al., 2001). Thus, the 5200 m estimated paleoelevation is likely an underestimate and not an overestimate at 15.1 Ma. The current elevation of the sample localities is ~4400 m, with surrounding elevations >5600 m, suggesting that there has been no discernible change in elevation since 15 Ma.

Our results based on $\delta^{18}O$ values can be compared with the estimates based on paleoenthalpy derived from floral physiognomy. Spi-

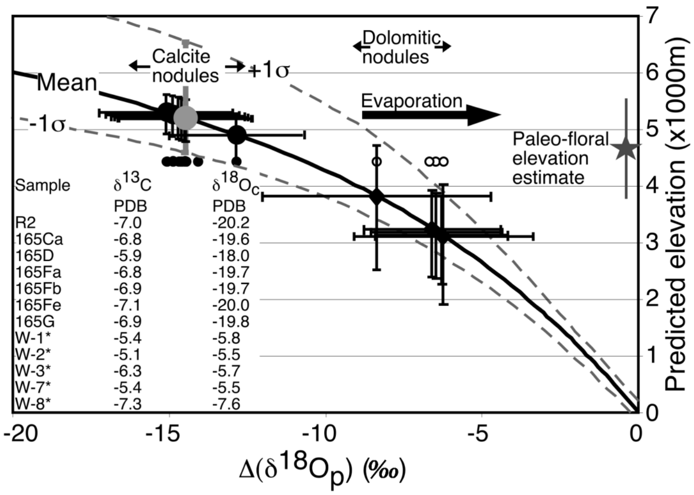

Figure 4. List of sample $\delta^{13}C$ and $\delta^{18}O_c$ values (c—carbonate; PDB—Peedee belemnite, asterisk—dolomitic nodules) and graph of $\Delta(\delta^{18}O_p)$ vs. predicted elevation for Oiyug Basin samples. Solid black curve is $\Delta(\delta^{18}O_p)$ vs. mean predicted elevation; dashed curves above and below correspond with $+1\sigma$ and -1σ model-derived uncertainties of elevation, respectively, from Rowley et al. (2001). Small circles are modern elevations of sample localities (filled—calcitic, open—dolomitic). Large black-filled circles—estimated $\Delta(\delta^{18}O_w)$ values of calcite nodules. Black-filled diamonds—estimated $\Delta(\delta^{18}O_w)$ values of dolomitic nodules described in text. Larger gray-filled circle—average $\Delta(\delta^{18}O_w)$ value of calcitic nodules. Black horizontal lines—uncertainties in $\Delta(\delta^{18}O_w)$ values based on combination of uncertainties in temperature of fractionation and mean low-elevation isotopic composition of precipitation. Black vertical lines—uncertainties of mean elevation corresponding with uncertainties in $\Delta(\delta^{18}O_w)$ values. Thicker gray vertical line through calcite nodule average—uncertainty from Rowley et al. (2001). Gray star—paleoelevation estimate and uncertainty from Spicer et al. (2003) based on floral physiognomy placed arbitrarily on $\Delta(\delta^{18}O_w)$ axis.

cer et al. (2003) reported a paleoelevation of the basin floor where the floras lived of 4650 ± 875 m, which is analytically indistinguishable from the oxygen isotope–based estimate of 5200 m +340/−405 (Fig. 4). This represents the first time that two paleoaltimeters have been directly compared and they accord remarkably well.

CONCLUSIONS

Spicer et al. (2003) noted that their results, now supported using $\delta^{18}O$ values, imply that southern Tibet has remained at a high elevation for at least the past 15 m.y. This does not match model-based predictions (Harrison et al., 1992; Molnar et al., 1993) that Tibet would have had a mean elevation of ~3 km prior to ca. 8 Ma (associated with a near doubling of crustal and mantle lithosphere thickness) followed by an elevation increase ca. 8 Ma (due to the gravitational instability–induced detachment of the thickened mantle lithosphere). The lack of an elevation change since 15 Ma implies that lithospheric-mantle thickening, as envisioned in the modeling of Molnar et al. (1993), plays an as-yet indiscernible role during this continental collision. As such, models invoking mantle thickening and instability-driven detachment, if it did occur, do not appear to play a role in the development of topography and the kinematic evolution of the Himalaya-Tibet collisional system, as has been assumed. These results are in accord with predictions derived from thermo-mechanical models of a Himalayan-Tibet–style collision published by Beaumont et al. (2004). Currently available data from southern Tibet do not allow an assessment of when significant topography developed in this region; thus the longer-term evolution of topography in this part of southern Tibet remains unconstrained.

ACKNOWLEDGMENTS

We thank Jin Yugan of the Nanjing Institute of Geology and Paleontology, Academia Sinica, for arranging access and logistical support, and W.S.F. Kidd and Bin Zhu for assistance in the field. Dan Schrag graciously provided the water and isotopic measurements of carbonates reported in his paper. The manuscript was improved by the reviews of Peter Molnar and an anonymous reviewer. This work was supported by the National Science Foundation (grant EAR-9973222). Rowley acknowledges discussions with colleagues in the Canadian Institute for Advanced Research, Earth System Evolution Program.

REFERENCES CITED

Argand, E., 1924, La tectonique de l'Asie: Proceedings of the XIIIth International Geological Congress, Brussels, v. 1, part. 5, p. 181–372.

Beaumont, C., Jamieson, R.A., Nguyen, M.H., and Medvedev, S., 2004, Crustal channel flows: 1. Numerical models with applications to the tectonics of the Himalayan-Tibet orogen: Journal of Geophysical Research, v. 109, B06406, doi: 10.1029/2003JB002809.

Bin, Z., Kidd, W.S.F., Rowley, D.B., Currie, B.S., and Shafique, N., 2005, Age of initiation of the India-Asia collision in the eastern Himalaya: Journal of Geology (in press).

Brewer, R., 1976, Fabric and mineral analysis of soils: New York, Krieger, 482 p.

Calvo, J.P., Alonso Zarza, A.M., and García del Cura, M.A., 1989, Models of Miocene marginal lacustrine sedimentation in response to varied depositional regimes and source areas in the Madrid Basin (central Spain): Palaeogeography, Palaeoclimatology, Palaeoecology, v. 70, p. 199–214.

Cerling, T.E., and Quade, J., 1993, Stable carbon and oxygen isotopes in soil carbonates, *in* Swart, P., et al., eds., Continental indicators of climate: American Geophysical Union Geophysical Monograph 78, p. 217–231.

Dewey, J.F., and Burke, K.C.A., 1973, Tibetan, Variscan, and Precambrian basement reactivation: Products of continental collision: Journal of Geology, v. 81, p. 683–692.

Friedman, I., and O'Neil, J.R., 1977, Compilation of stable isotope fractionation factors of geochemical interest, *in* Fleischer, M., ed., Data of geochemistry: U.S. Geological Survey Professional Paper 440-K, 12 p.

Garzione, C.N., Dettman, D.L., Quade, J., DeCelles, P.G., and Butler, R.F., 2000, High times on the Tibetan Plateau: Paleoelevation of the Thakkhola graben, Nepal: Geology, v. 28, p. 339–342.

Harrison, T.M., Copeland, P., Kidd, W.S.F., and An, Y., 1992, Raising Tibet: Science, v. 255, p. 1663–1670.

International Atomic Energy Agency, 1992, Statistical treatment of data on environmental isotopes in precipitation: Vienna, International Atomic Energy Agency, 781 p.

Kelts, K., and Talbot, M.R., 1989, Lacustrine carbonates as geochemical archives of environmental change and biotic/abiotic interactions, *in* Tilzer, M.M., and Serruya, C., eds., Large lakes: Ecological structure and function: Berlin, Springer-Verlag, p. 288–315.

Machette, M.N., 1985, Calcic soils of the southwestern United States, *in* Weide, D.L., ed., Soils and Quaternary geology of the southwestern United States: Geological Society of America Special Paper 203, p. 1–21.

Mack, G.H., James, W.C., and Monger, H.C., 1993, Classification of paleosols: Geological Society of America Bulletin, v. 105, p. 129–136.

Molnar, P., England, P., and Martinod, J., 1993, Mantle dynamics, uplift of the Tibetan Plateau, and the Indian Monsoon: Reviews of Geophysics, v. 31, p. 357–396.

Rowley, D.B., Pierrehumbert, R.T., and Currie, B.S., 2001, A new approach to stable isotope–based paleoaltimetry: Implications for paleoaltimetry and paleohypsometry of the High Himalaya since the late Miocene: Earth and Planetary Science Letters, v. 188, p. 253–268.

Spicer, R.A., Harris, N.B.W., Widdowson, M., Herman, A.B., Guo, S., Valdes, P.J., Wolfe, J.A., and Kelley, S.P., 2003, Constant elevation of southern Tibet over the past 15 million years: Nature, v. 421, p. 622–624.

Manuscript received 8 September 2004
Revised manuscript received 9 November 2004
Manuscript accepted 11 November 2004

Printed in USA